Screen-Printed Carbon Electrodes

Stephen Fletcher

Department of Chemistry, Loughborough University, Ashby Road,
Loughborough, Leicestershire LE11 3TU, UK.

E-mail: ProfSFletcher@Virginmedia.com

Book Chapter Published 14 October 2015.

Please cite as:
Stephen Fletcher, Screen-Printed Carbon Electrodes, in *Electrochemistry of Carbon Electrodes* (Edited by Richard C. Alkire, Philip N. Bartlett and Jacek Lipkowski), Wiley-VCH Verlag GmbH & Co. KGaA, Weinheim, Germany, pp 425-444 (2015).
doi: 10.1002/9783527697489.ch12

Keywords/Index

Conductivity of composites; carbon polymorphs; oxygen functionalities; activated carbons; binder-solvent combinations; PVDF properties; PVDF solubility; flexible substrates; screen-printing process; screen printing materials; ink flow; substrate wetting; commercial ink additives; binder percentage; multi-layered electrodes; *IR* drop; areal capacitance, equivalent circuit.

Introduction

Over the past twenty years, the screen printing of electrodes and sensors has emerged as a major branch of electrochemical research, with hundreds of documents being published which refer to the technique or which claim to apply it in a novel way [1-13]. During the same period, numerous screen-printing techniques have also been adapted for electronic circuit fabrication, and today these form an essential part of a multi-billion dollar industry. The great driving force for these historical advances has been the realization that screen printing can be much cheaper to implement than traditional methods of manufacturing. Given this insight, and the continuing need for miniaturization of advanced electronics, the time is perhaps ripe to take stock of these developments, and to collate some of the fundamental science behind this revolution in print technology. As a small contribution towards this goal, I here review certain physical and chemical aspects of the screen printing process relevant to the manufacture of carbon electrodes.

Screen printing provides the possibility of manufacturing large numbers of carbon electrodes in a reproducible, low-cost, and disposable format. It also permits the incorporation of chemically functionalized materials in a straightforward way. Currently, screen-printed carbon electrodes find application in many areas of electrochemistry, but most notably in chemical and biochemical sensing, energy conversion and storage, and microelectronics. They also find application in flexible electronics, which is a rapidly-developing technology for printing electronic devices directly onto flexible plastic substrates, such as polycarbonate, polyimide, and PEEK. Almost all forms of carbon have been deposited by screen printing, with graphite, carbon black and activated carbon being the most widely used. Other forms of carbon that are the subject of continuing interest include carbon nanotubes, carbon nanofibres, and graphene.

The screen-printing process has three principal advantages over other methods of electrode manufacture. Firstly, the electrode area, electrode thickness, and electrode composition are readily controlled. Secondly, statistical validation of experimental results is made possible by the existence of replicate electrodes. Thirdly, catalysts can be incorporated simply by adding them to the screen-printing ink (paste). The main disadvantage of screen printing is that it is restricted to flat substrates.

For electrochemical purposes, the chemical composition of the ink is paramount. Three components are absolutely essential: a conducting filler, a non-conducting binder, and a volatile solvent. After the ink is printed, the volatile solvent evaporates, leaving behind the conducting filler cemented into the binder. This process is known as “curing”. During curing, the binder may simply precipitate from solution, or it may polymerize depending on its composition. Because some solvent residue inevitably contaminates the final product, the first rule of ink formulation is to ensure that the solvent is electrochemically inactive over a wide range of electrode potential (i.e. has a wide “electrochemical stability window”). The solvent must also be free of non-volatile impurities. Preferably, it should also be non-toxic.

The ideal finished product of the screen-printing process is a solid composite system consisting of small particles of conducting filler (such as particulate graphite) uniformly dispersed inside an inert binder (such as a sigma-bonded polymer). Within the bulk of the composite, each particle of conducting filler must be physically located within electron tunnelling distance of its neighbour (~1.4 nm) otherwise it will not contribute to the long-range conductivity of the total electrode. To ensure this latter criterion is met, very high volume fractions of conducting filler must be incorporated inside the composite (>64% for random close packing of spherical particles of the same size) [14, 15], and of course the spatial dispersion of the filler particles should be as statistically homogeneous as possible. The detailed relationship between the bulk conductivity of composites and their three-dimensional structure is the province of *Percolation Theory* [16]. According to the latter, smaller volume fractions of conducting filler can be tolerated if the filler consists of non-spherical particles such as platelets or long thread-like chains.

Conductivity of Composites

In order to enhance the conductivity of printed electrodes, ink slurries are commonly pulverized in ball mills. This process creates very small particles of conducting carbon known as “fines” (1-100 nm diameter) which, after printing, bridge the electron tunnelling gaps between the larger particles. However, since milling always causes some attrition of the mill surface, the mill interior should be made of agate (a cryptocrystalline variety of silica), rather than stainless steel, in order to prevent the introduction of trace amounts of iron and

chromium. An alternative method of enhancing the conductivity of printed electrodes is to add small quantities of carbon black to the test ink (typically 5-15% by weight of solids, depending on micromorphology) [17]. Carbon black is the generic name for a family of small-particle carbon powders which are formed in the gas phase by thermal decomposition of hydrocarbons. Carbon blacks are commercially available in a wide variety of grades, which differ in the size and shape of their particles and the chain-length of their aggregates. Different grades may also have different degrees of compaction.

When carbon black is used in the laboratory, it must be handled with great care because of its potentially adverse effects on human health. The safest type of carbon black is *acetylene black*. This consists of graphitized particles, usually between 8 nm and 80 nm diameter, aggregated into long chains, having a specific surface area of ~60 m^2/g. After printing, the long chains lower the percolation threshold of the conductivity network without introducing toxic impurities. More hazardous types of carbon black are *furnace blacks* which contain carcinogenic compounds such as polycyclic aromatic hydrocarbons (PAHs), and *thermal blacks* which contain aggregates in the size range 1-5 µm which may become trapped in human lungs. Regardless of provenance, however, inhalation of all carbon blacks should be strictly avoided.

Carbon Polymorphs

Just after the Second World War, Rosalind Franklin famously classified carbons as either "graphitizing" or "non-graphitizing", depending on their ability to form graphite in response to high-temperature heat treatment [18]. By means of x-ray diffraction, she observed that graphitizing carbons had very few sp^3 defects, thus allowing them to form extended sp^2 layer planes. In contrast, non-graphitizing carbons (such as glassy carbons, activated carbons, and high-modulus carbon fibres) had large amounts of tetrahedral sp^3 bonding trapped inside their structures, and hence were structurally rigid.

Since Franklin's time, many new polymorphs of carbon have been discovered, and today these are generically classified as *foliated* (graphite and its intercalation compounds), *exfoliated* (graphene and graphene oxide), or *hierarchical* (carbon black). On the atomic

scale, some remarkable valence-satisfying structures have also been discovered, such as icosahedra (fullerenes), cylinders (nanotubes), and semi-infinite sheets (graphenes). Stress-relieving pentagonal and heptagonal carbon rings have also been observed. Adding to this super-abundance of morphologies, many important carbon materials also display oxygen functionalities on their surfaces, either as remnants from their synthesis or as deliberately introduced features. In extreme cases, oxygen/carbon ratios may exceed 10% w/w.

Oxygen Functionalities

Carbon forms two different types of covalent bond with oxygen. A carbon-oxygen single bond contains one sigma bond and no pi bonds, whereas a carbon-oxygen double bond contains one sigma bond and one pi bond. The pure sigma-bond motif is found in C–OH groups (as seen in phenols) while the mixed sigma/pi motif is found in C=O groups (as seen in carbonyls and quinones). Thus, the oxygen atoms in C–OH groups are sp^3 hybridized, whereas the oxygen atoms in C=O groups are sp^2 hybridized.

Some oxygen functionalities are redox active, such as carbonyl and quinone. Others respond to pH, such as carboxylate (aqueous pK_a ~4) and phenolic-hydroxide (aqueous pK_a ~10). Yet others are comparatively inert, such as lactone and ether. In all cases, however, oxygen functionalities occur more frequently on edge planes than basal planes, due to the termination of the graphitic lattice there. In the carbon industry, it has long been recognized that the hydrophilicity of carbon surfaces can be enhanced by the introduction of oxygen functionalities. Similarly, the wettability of pores inside bulk carbon can be improved by internal oxidation. The explanation of both effects is that oxygen atoms behave as negatively charged loci for hydrogen bonding to water molecules.

Oxygen functionalities are notoriously difficult to remove. To a first approximation, the C–OH functionality has a carbon-oxygen bond strength of ~350 kJ/mol, while the C=O functionality has a carbon-oxygen bond strength of ~745 kJ/mol. These values are very high, and they prevent the pyrolytic elimination of carboxylate groups until $T > 600$ °C, and the pyrolytic elimination of quinone groups until $T > 1000$ °C.

Activated Carbons

Historically, almost all forms of carbon have been used in the screen-printing process. In recent times, however, activated carbons have aroused special interest because of their potential applications in batteries and supercapacitors. Industrially, activated carbons are synthesized from organic matter such as charcoal, wood, peat or coconut shells. This typically involves a two-step process: (i) *carbonization* in which the parent material is pyrolysed in a reducing atmosphere in the range 600-1200 °C, then (ii) *activation* in which the initial product is surface oxidized by oxygen, carbon dioxide, or steam in the temperature range of 600-1200 °C. Provided the starting material resists full graphitization, the original porous structure of the organic matter is retained by the final product, typically yielding a notional B.E.T. specific surface area in the range 500 to 1500 m^2/g for particles of 15 μm diameter. At the other extreme, mesophase carbon microbeads (MCMBs), which also consist of particles of 15 μm diameter, exhibit notional B.E.T. specific surface areas of only 1 to 3 m^2/g. These are used as intercalation hosts in lithium ion batteries.

Within the supercapacitor industry, it is widely speculated that stand-alone screen-printed carbon electrodes might one day attain equivalent-series gravimetric capacitances of ~100 F/gm (based on the total mass of carbon, binder and ion-supplying solution), and equivalent-series volumetric capacitances of ~150 F/cm^3 (based on the total volume of carbon, binder and ion-supplying solution). However, at the present time, commercial electrodes typically attain less than half these figures. Even smaller equivalent-series gravimetric capacitances (10-50 F/gm) are obtained from oxidized nanotubes, chopped nanofibres, and carbon aerogels. In general, the best electrode responses correlate with highly oxidized carbon materials, well-conducting electrolytes, slit-shaped micropores, long charging times (minutes), and thin films (<500 μm). For a 125 μm film of activated carbon, one finds a maximum equivalent-series areal capacitance of ~1 F/cm^2 (where the area is defined as the convex hull of the electrode). Methods of increasing this number would be of great interest to the supercapacitor industry. On the other hand, for sensors, *minimum* equivalent series capacitance densities are also sought by analytical chemists, and these values may be as low as ~100 $\mu F/cm^2$ in the case of non-porous, oxygen-free, particulate graphite.

Binder/Solvent Combinations

Over the years, innumerable binder/solvent combinations have been trialled in screen printing formulations, but few successful compositions have been disclosed in the open literature. This is because of their commercial value. Nevertheless, it is clear that two different kinds of polymeric binder are in widespread use, *thermoplastic* and *thermosetting*. Among electrochemists, perhaps the most popular approach is to dissolve a thermoplastic polymer in a high-boiling solvent. Representative systems of this type are poly(vinylidene fluoride)/*N*-methyl-2-pyrrolidone (PVDF/NMP), poly(carbonate)/solvent-naphtha (PC/SN), poly(methyl methacrylate)/ethylene glycol diacetate (PMMA/EGDA), poly(sulfone)/dimethylacetamide (PS/DMAC), and ethyl cellulose/α-terpineol (EC/AT). The main advantage of using a thermoplastic polymer as a binder is that it has a low degree of cross-linking, which makes the finished product slightly flexible. At the other extreme, various thermosetting systems have also been developed, based mainly on acrylic-melamine and epoxy resin formulations, and these create more brittle films. A shortcoming of thermosetting systems is their high initial reactivity, although this usually fades with time due to the formation of covalent cross-links during curing. The diglycidyl-ether of bisphenol-A (DGEBA) is a particularly popular cross-linking agent in epoxy resins. It is formed by reaction of bisphenol-A with epichlorohydrin in the presence of a basic catalyst.

Although they are widely available as components of complex commercial products, thermosetting binders are difficult to obtain pure. For example, acrylic-melamine formulations almost always contain mixtures of industrial solvents as diluents (such as 2-heptanone and *n*-butanol), and they may also contain proprietary dispersing and wetting agents. Similarly, epoxy resin formulations commonly contain industrial xylene and/or methyl isobutyl ketone as diluents, plus silicones and wetting agents. Plasticizers such as dioctyl phthalate are also widely used to decrease viscosity, despite being suspected endocrine disruptors. The many and various consequences of including these ingredients should be carefully considered before scientific use. It should also be noted that the maximum operating temperature of epoxy-based carbon electrodes is 120 °C. Their surfaces also swell in small-molecule organic solvents.

Among thermoplastic binders, polyvinylidene fluoride (PVDF) is probably the most widely-used. It is a partially fluorinated polymer produced by the polymerization of 1,1-

difluoroethylene, and typically has a molecular weight in the range 180,000 to 550,000 Da. Commercially, PVDF is synthesized by two different routes: *emulsion polymerisation* and *suspension polymerisation*, with the emulsion-polymerized PVDF having the smaller particle size. Hence it is easier to dissolve. The customary solvent for PVDF is *N*-methyl-2-pyrrolidone (NMP). After printing and curing, PVDF-bound electrodes are resistant to many room-temperature solvents, acids and bases. In recent years, PVDF has also emerged as the industry standard binder in lithium ion batteries, partly because its high molecular weight improves the adhesion of electrode components.

Polycarbonate is another binder used in screen-printing formulations. It typically has a molecular weight in the range 20,000 to 200,000 Da and is attractive because it can undergo large plastic deformations without cracking or breaking. Unfortunately, it also contains potentially harmful traces of bisphenol-A. Complicating matters still further, the standard solvent for polycarbonate is solvent-naphtha, which contains a complex mixture of aromatic hydrocarbons. Fortunately, solvent-naphtha can be replaced by 1,2,4-trimethylbenzene when high purity is required. Poly(methyl methacrylate) (PMMA) and poly(styrene-co-methyl methacrylate) are practical alternatives to polycarbonate, but more brittle. They do not contain the potentially harmful bisphenol-A subunits found in polycarbonate, and can be dissolved in ethylene glycol diacetate (EGDA). The latter is a slow-evaporating bio-degradable solvent (bp 190 °C) that is used in some commercial lacquers and enamels. Polysulfone belongs to a lesser-known family of thermoplastic polymers that is able to function continuously at temperatures up to 160 °C. Commercial polysulfone has a molar mass of ~35,000 Da and a glass transition temperature of ~190 °C. This polymer is customarily dissolved in dimethylacetamide (DMAC) or butyrophenone, and finds use in carbon and silver inks. In addition, it has been recommended for use in electrochemical nanobiosensors [19]. Finally, ethyl cellulose is a derivative of cellulose in which some of the hydroxyl groups on the anhydro-glucose units have been converted into ethyl ether groups. It is practically insoluble in water, but dissolves in α-terpineol (bp 217 °C). It is used in the manufacture of some gas sensors, and to form carbon catalyst layers in dye-sensitized solar cells [20].

PVDF Properties

For general electrochemical measurements there are many powerful constraints on the choice of binder. In addition to supplying a strong adhesive bond to the conducting filler, and a strong cohesive bond inside itself, the binder must also be wettable by water (i.e. exhibit a contact angle < 90°). It should also have a wide electrochemical stability window, a high purity, and be insoluble in a wide range of common solvents. For all of these reasons, poly(vinylidene fluoride) (PVDF) is a good choice. It is a partially-fluorinated semi-crystalline polymer with excellent electrochemical and thermo-mechanical properties. In particular, it is electrochemically stable in the range 0 to +5 V *vs* Li/Li^+, it exhibits no thermal degradation below 300 °C, and its volume resistivity is $\geq 10^{14}$ ohm cm.

To a first approximation, PVDF can be thought of as a bulk combination of two components, a high-density crystalline component and a low-density amorphous component. The observed density (ρ) of a given specimen is then given by the formula

$$\rho = f_{\text{crys}}\rho_{\text{crys}} + f_{\text{amorph}}\rho_{\text{amorph}}$$

where f_{crys} is the volume fraction of the crystalline component, ρ_{crys} is the density of the crystalline component (g/cm^3), f_{amorph} is the volume fraction of the amorphous component and ρ_{amorph} is the density of the amorphous component (g/cm^3). For a typical commercial PVDF,

$$\rho_{\text{amorph}} \approx 1.68\ \text{g/cm}^3$$

$$\rho_{\text{crys}} \approx 1.88\ \text{g/cm}^3$$

and

$$f_{\text{amorph}} \approx 60\%$$

$$f_{\text{crys}} \approx 40\%$$

yielding a density of ~1.76 g/cm³ (as observed). This is almost twice the value of high-density polyethylene (0.93 g/cm³). From a mechanical point of view, the crystalline component imparts rigidity to the binder, while the amorphous component imparts elasticity. The crystallinity also affects the melting point. The crystalline component melts sharply at 177 °C, whereas the amorphous component melts gradually over the range 165-175 °C.

It is well known that, in the absence of surfactants, fully fluorinated polymers such as poly(tetrafluoroethylene) (PTFE) and poly(perfluoroalkoxy ethylene) (PFA) cannot be wetted by polar solvents. For this reason, they are not recommended as binders for screen-printed electrodes (although they do find specialist use in gas diffusion electrodes and in lithium thionyl chloride batteries). The physicochemical origin of their non-wettability lies in the fact that their fluorine atoms are densely packed together, so that their surface dipole is zero. By contrast, poly(vinylidene fluoride) (PVDF) displays alternating CF_2 and CH_2 units at its surface, which allows the highly electronegative fluorine atoms to extract electrons from the nearby hydrogen atoms. The resulting surface dipoles interact strongly with nearby solvent molecules through dipole–dipole coupling and hydrogen bonding. As a result, PVDF is surprisingly wettable by water (contact angle ~80°).

Unfortunately, if left in laboratory air for any length of time, PVDF surfaces tend to adsorb solvophobic impurities. As a result, aged electrodes containing PVDF may sometimes be difficult to wet with electrolyte solution. In such cases, the natural wettability of PVDF can be restored by pre-wetting the printed electrodes with isopropyl alcohol (IPA) or by adding surfactants to the electrolyte solution. Poor wettability is also a problem with PVDF copolymers such as PVDF-HFP, poly(vinylidene fluoride-*co*-hexafluoropropylene), which is sometimes used as an alternative to pure PVDF when enhanced flexibility is needed. Although the pendant trifluoromethyl groups ($-CF_3$) of HFP successfully disrupt the crystalline regions of the PVDF, making it more ductile, they also impart greater solvophobicity. At the same time, the melting point of the copolymer falls by about 3 degrees Celsius for each 1% of HFP added.

PVDF Solubility

One of the paradoxes of screen printing is that the binder material must not dissolve in any of the common solvents used in electrochemistry, but must dissolve in at least one solvent to create the printing ink. This enigmatic requirement is actually met by PVDF. It is insoluble in solvents having low Hildebrand solubility parameter ($\delta_H < 20$ $MPa^{1/2}$) such as hydrocarbons, perfluorinated solvents, ethers and glymes, and it is also insoluble in solvents having high

Hildebrand solubility parameter (δ_H > 28 MPa$^{1/2}$) such as water and alcohols. However, it does dissolve in an elite group of solvents that have intermediate Hildebrand solubility parameters (in the range δ_H = 20-28 MPa$^{1/2}$). A list of these is given in Table 1. What all of these solvents have in common is that they have large dipole moments and weak internal hydrogen bonding – just like PVDF itself. The solubility parameters of poly(vinylidene fluoride) have been summarized by Bottino et al [21].

Table 1. Halogen-free, high-boiling solvents for PVDF.
(δ_H is the Hildebrand solubility parameter.)

		mp (°C)	bp (°C)	Dipole Moment (debye)	δ_H (MPa$^{1/2}$)	Flash Point (°C)
Propylene carbonate	PC	−49	242	4.98	27.2	132
Hexamethylphosphoramide	HMPA	+7	230	5.38	23.2	106
Gamma butyrolactone	GBL	−45	204	4.27	26.2	98
N-methyl-2-pyrrolidone	NMP	−24	202	3.92	22.9	86
Dimethylsulfoxide	DMSO	+16	189	3.96	26.7	85
Isophorone	IP	−8	214	3.96	20.0	84
Acetophenone	AP	+19	202	3.15	20.8	82
Tetramethylurea	TMU	−1	177	3.44	21.7	66
N, *N*-dimethylacetamide	DMAC	−20	165	3.81	22.7	63
N, *N*-dimethylformamide	DMF	−61	153	3.86	24.8	58
Cyclohexanone	CH	−47	155	3.25	20.2	47

Flash points mainly from WolframAlpha [22]. Hildebrand values mainly from ref [23]. Other data from refs [24] and [25]. **Warning**: hexamethylphosphoramide and isophorone are confirmed animal carcinogens. **Warning**: DMF and NMP are suspected embryotoxins.

In principle, any of the solvents listed in Table 1 could be used to manufacture PVDF-based inks. However, because the curing of carbon inks typically takes place at T > 110°C (to ensure the removal of water and other volatile impurities) most of the listed solvents find themselves evaporating above their flash points. The flash point of a solvent is defined as the lowest temperature at which its equilibrium vapour will ignite in air. As a consequence, only propylene carbonate can be evaporated with complete thermal safety. Further advantages of propylene carbonate are that (i) it has a mild odour, (ii) it is not strongly hygroscopic, and (iii) it is non-toxic by inhalation [26]. By contrast, the more widely used NMP has an amine-like odour, is strongly hygroscopic, and is a suspected human reproductive hazard [27]. As regards electrochemistry, the electrochemical stability window of propylene carbonate

containing 0.1 M $LiClO_4$ as supporting electrolyte extends from –3.2 V to +2.6 V (*vs* Fc/Fc^+), which is highly attractive for general electrochemical purposes.

At room temperature, the rate of dissolution of semi-crystalline PVDF is slow in all known solvents, even though its glass transition temperature is −35 °C, and even though the free energy of mixing is negative. The reason for this reluctance to dissolve is the high density of the crystalline material, which kinetically hinders the ingress of solvent molecules. As a result, the solvent/PVDF mixture must be maintained at $T > 60°C$ for at least three days to ensure that the dissolution of PVDF proceeds to completion. Lower temperatures and shorter dissolution times may result in the formation of gels. In gels, sub-micrometre remnants of the crystalline polymer remain undissolved [28]. To help avoid gel formation, the solvent should also be scrupulously dried, since a few percent of water can also cause gelling.

For laboratory use, each solvent in Table 1 can be dried inside a burette containing a mixture of thermally activated carbon and Type 3A molecular sieve. This not only removes trace impurities but also greatly diminishes the free water content (typically below 30 ppm after 24 hrs). Alternatively, if the solvents are badly contaminated with impurities, they should first be dried by molecular sieve, decanted, and then distilled under inert atmosphere prior to use. [**Warning**: Never distil solvents to dryness.] PVDF powder can be dried at 110°C in a vacuum oven (2 mbar) for 24 hr before use.

Flexible Substrates

Flexible substrates for screen-printed electrodes must meet a range of demanding requirements, especially for display applications. Besides the most obvious requirement – low flexural rigidity – they also need high temperature stability, high solvent resistance, good optical clarity, micro-rough surface texture (± 50 nm), and low cost.

In general, however, the most important requirement is low flexural rigidity (low bending stiffness) D ($N \cdot m^2$). From an engineering perspective, this is related to the first power of the tensile modulus and the third power of the substrate thickness,

$$D = \frac{Ebh^3}{12(1-\mu^2)}$$

Here E is the tensile modulus (Young's modulus, N/m^2), b is the substrate width, h is the substrate thickness, and μ is Poisson's ratio for the substrate material (0.3-0.5). In the absence of an exact value of the latter, it may be assumed to be $\mu \approx 0.5$, since this gives the worst-case value (highest value) of flexural rigidity. Evidently, the third power dependence on h makes the substrate thickness the most important parameter in the system.

Widely used substrate materials include poly(ethylene naphthalate) and poly(ethylene terephthalate) of thickness 25-75 micrometres. A cheap commercial source of poly(ethylene terephthalate) is laser inkjet transparency film. Interestingly, both PEN and PET can withstand temperatures up to 180-220 °C. PEN also has the advantage that it is about three times less permeable to water and oxygen than PET. Other widely used substrate materials include polycarbonate, polyimide, and PEEK. Some commercial plastic films are also obtainable with oxygen plasma-treated poly(urethane) primer layers on one side, to raise the surface energy and thereby improve the adhesion of inks.

Screen-Printing Process

The screen printing process is actually a type of stencilling, in which the carbon ink is forced through the open regions of a mesh screen to form a pattern on a surface. When viewing the process for the first time, most people imagine that the entire image is deposited simultaneously. However, the mesh screen actually stops 1-2 mm above the substrate, and the two come into contact only when the edge of a poly(urethane) "doctor blade" [a corruption of *ductor* blade] sweeps over them. This prevents the screen and the substrate from sticking together. Figure 1 is a simplified representation of the screen-printing process.

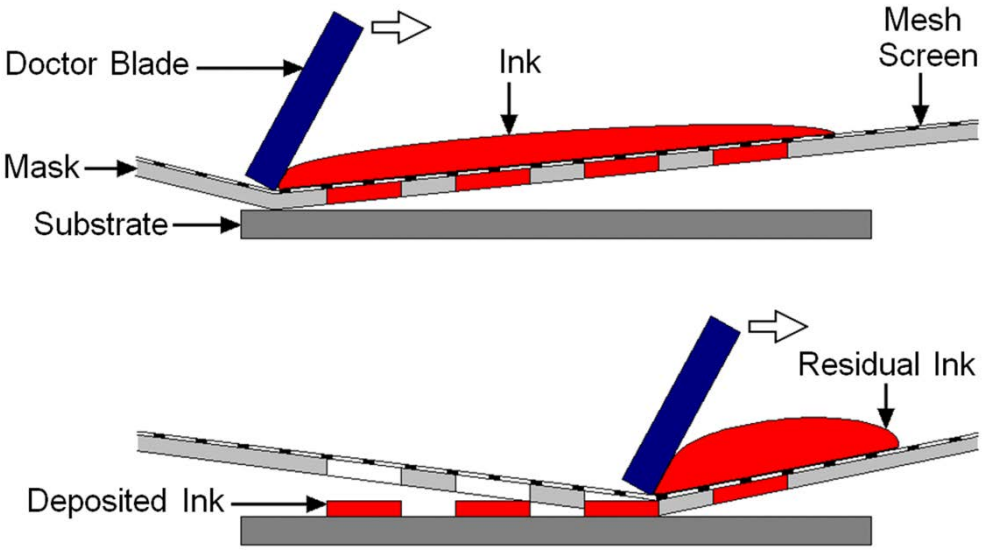

Figure 1. *The Screen-Printing Process. (From N. J. van Dijk [29])*

Screen Printing Materials

Screen printing uses mesh screens to support the ink prior to its extrusion onto the substrate. Three mesh materials are in common use: steel, polyester, and nylon. However, steel is preferred for making thick carbon electrodes because it possesses a greater open area, and thus allows more ink to transfer for each pass of the doctor blade. Steel is also very resilient, readily resuming its original position after the passage of the doctor blade.

Ink-free regions in the image are created by coating the mesh with a "mask" made of a rubbery ink-repelling, polymer, usually poly(vinyl acetate). This mask defines the shape of the image by providing a boundary for the ink. The reproducibility of the printed image depends on the mesh's ability to form a gasket-like seal with the substrate when the doctor blade passes over it. In the laboratory, mask thickness and screen mesh size are commonly chosen by trial-and-error. The hole size and the wire diameter determine the thickness of the printed layer, while the wire spacing determines the resolution (and hence reproducibility) of the printed area. A physical model of the screen printing process has been described by Owczarek and Howland [30].

The screen mesh size is conventionally characterized by the number of wire strands per centimetre (spc), so larger spc values imply finer detail. High definition stainless steel screens typically have 180 strands per centimetre, creating apertures of 45 μm for strand diameters of 10 μm. To prevent screen blockage during printing, the maximum particle diameter should therefore be about one-third this value (~15μm). Particles above 20 μm can be removed by preliminary dry sieving. Mesh tensions are usually set around 30 N/cm, and printed film thicknesses are typically in the range 15 to 150 μm.

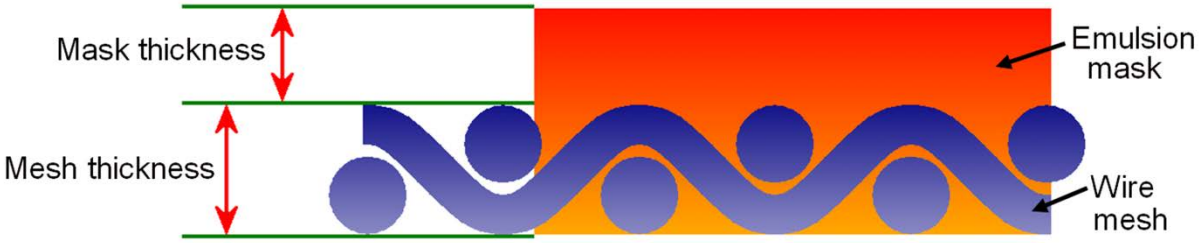

Figure 2. *Mesh and mask geometry*

In practice there is a limit to layer thickness (and hence mask thickness) determined by the tendency of thick layers to crack during drying. At the other extreme, very thin layers tend to have high electrical resistance. After use, most screens can be safely cleaned with volatile esters (butyl acetate, ethyl acetate) or ketones (methyl isobutyl ketone, methyl ethyl ketone).

Ink Flow

From a colloid science point of view, carbon inks are two-phase gels. They consist of structured networks of solid particles thoroughly permeated by a polymer solution. As two-phase gels, they behave as classic non-Newtonian fluids, and commonly exhibit a decreased viscosity upon the application of a finite shear stress (thixotropy). The original viscosity is restored only after the shear stress is removed. Although thixotropy is a nuisance in many industrial processes, screen printing actually *requires* inks to be thixotropic. The reason for this is as follows. When first placed on the mesh screen, the ink must be so viscous that it remains immobile. Then, as the doctor blade passes over it, it must become so non-viscous that thousands of tiny droplets of ink extrude through the mesh and spread over the substrate.

Finally, after the droplets have coalesced, the viscosity of the ink must rise again, in order to preserve the shape of the transferred image.

Because screen-printing inks are thixotropic, they have a natural tendency to gel during storage. In most cases this can be rectified by stirring (though not so vigorously that air bubbles are introduced). The optimum ink viscosity at the start of the screen-printing process depends on the design parameters of the screen printer, but is generally about 10^3 poise ($= 10^5$ mPa s). Note, however, that an initial viscosity of this magnitude is no guarantee that a particular ink will print well, because it may not be shear-thinning enough to pass through the screen [31]. At a shear rate ($\dot{\gamma}$) of 10 s^{-1} (typical for a carbon ink passing through a steel mesh screen) the viscosity should fall to about 10 poise ($= 10^3$ mPa s).

Substrate Wetting

In order for a solvent to wet a substrate, its surface energy (surface tension) must be lower than that of the substrate. Since many common substrates such as polyester, polyimide, and polyacrylate all have surface energy values around 45 dynes/cm, screen-printing solvents are normally chosen to have surface tension values around 40 dynes/cm. In this context, it should be noted that some common laboratory lubricants, such as silicone oils, have ultra-low surface energy values (< 22 dynes/cm) which means they will impair screen-printing quality if they contaminate a substrate.

The achievement of proper wetting is particularly problematic. There are only two ways of overcoming the failure of an ink to wet a substrate. One is to increase the surface energy of the substrate; the other is to decrease the surface energy of the ink. The surface energy of a substrate may be increased by oxygen plasma treatment to introduce polar functionalities. Alternatively, the surface energy of the ink may be decreased by the addition of surfactants. However, surfactants are a nuisance in many electrochemical systems. They aggregate in solution, adsorb at interfaces, and inhibit some electron transfer reactions. Indeed, the presence of surfactants in many commercial inks is a serious problem that is often overlooked by academic researchers. For biomedical applications, it should also be noted that some

surfactants are endocrine disruptors, and therefore are not approved by the U.S. Food and Drug Administration (FDA).

The ability of an ink to resist detachment after deposition is known as “tack”. Tack is influenced by many different factors, both intrinsic and extrinsic. Intrinsic factors include (i) the surface energies of ink and substrate, (ii) the viscoelasticity (cohesive strength) of the ink, and (iii) the surface roughness of the substrate. Extrinsic factors include (iv) the printing force, (v) the contact time, and (vi) the ambient temperature.

Tack is quantifiable as the work per unit area needed to dis-bond an ink immediately after adhesion. This is given by the formula

$$w = \frac{1}{A} \int F \cdot v \, \mathrm{dt}$$

where A is the geometrical contact area, F is the tensile force applied to the dis-bonding process, and v is the rate of separation. The work w (also known as the "adhesive failure energy") was originally developed by Gent, Kinloch, and Andrews [32-34] to quantify the strengths of adhesives. Good tack is important in the screen printing process because inks must resist pull-away as the mesh screen relaxes. On the nanometre scale, tack is generated in a patch-wise manner by the formation of multiple molecular contacts between the polymer binder and the substrate. Unsurprisingly, therefore, the greater is the contact time, the greater is the number and size of adhesive patches, and the better the resulting tack.

Commercial Ink Additives

Commercial screen-printing inks contain diverse mixtures of additives, including pigments, plasticizers, surfactants, extenders, dispersants and waxes. Pigments are used to control colour. Plasticizers are used to soften binders and improve the flexibility of the finished product. Surfactants are used to decrease the surface tension of the solvent. Extenders are used to lower cost. Dispersants are used to avoid particle coagulation, and waxes are used to improve the rub resistance and gloss of the finished product. All these additives are undesirable in electrochemistry and should be excluded from carbon inks.

Binder Percentage

Both laboratory experiments and computer simulations have shown that the random close packing of equally-sized, spherically-shaped, particles occupies a volume percentage of 64%. It follows that, if we want to eliminate porosity in such a system, then we must fill the remaining 36% of space (the "dead volume") with an inert binder. In contrast, if we want to retain some porosity, then a certain fraction of the dead volume must be kept free of binder. Based on a 50/50 compromise between electrode cohesion and solution access, one may therefore reasonably conjecture that the volume percentage of inert binder should be *circa* 18%, and indeed this is a good starting point in the laboratory development of porous electrodes from equally-sized, spherically-shaped, particles.

Of course, lower volume percentages of inert binder can be used if some of the dead volume is packed with smaller particles of the conducting material (fines). Indeed, if the fines are equally-sized among themselves, then the revised dead volume falls to 13% (i.e. 36% of 36%) and the volume percentage of inert binder that is needed to create a functioning porous electrode falls to 6.5%. At the other extreme, a volume percentage of binder higher than 18% could conceivably be used, but this would also increase the electrical resistance of the electrode.

Multi-layered Electrodes

The basic elements of a multi-layered electrode are shown in Figure 3. Each part has its own design specification, depending on end use. First, electrode materials have to withstand both oxidizing and reducing conditions. Second, total electrode resistance should be below $10\,\Omega$ to minimise errors associated with *IR* drop. Third, electrodes must have electroactive areas which are reproducible within 5% coefficient of variation. Fourth, during manufacture, all materials must withstand repetitive thermal cycling to $T > 110°C$. Fifth, all the electrode materials must be mutually adhesive. Sixth, there has to be a complete absence of electroactive impurities.

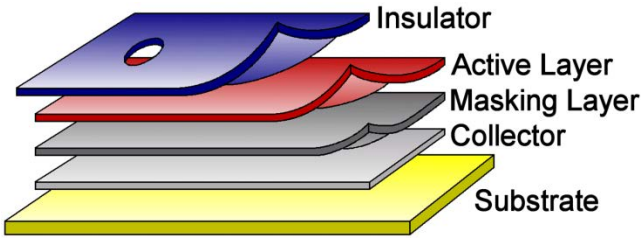

Figure 3. *The basic elements of a multi-layered electrode*

In addition to the above criteria, an insulator may be used to mask the final electrode layer and to define the size of the geometric area exposed to the solution. This insulator must be viscous enough not to creep (in order to create a well-defined electrode area) yet it must flow evenly under the pressure of the doctor blade to ensure good coverage. It must also be very pure. Preferably, it should also have a thermal expansion coefficient close to that of the printed ink, to prevent dis-bonding of the printed layers.

IR Drop

The electrical resistance of printed carbon electrodes made from standard commercial inks is about 50 ohms per cm, for a one-centimetre-wide strip. Since practical test cells typically require a contact strip at least 5 cm long, this implies an *IR* drop of circa 250 mV for a 1 mA current. For voltammetric work this is completely unacceptable. To overcome this problem a well-conducting silver layer is usually printed underneath the active layer. This decreases the total resistance to below 0.5 ohms per cm, but makes it necessary to block the unwanted electrochemistry associated with the silver surface. This latter is readily achieved by over-printing the silver layer with a layer of non-porous graphite secured with an epoxy binder. A scanning electron microscope image of a cross-section of an electrode of this type is shown in Fig. 4.

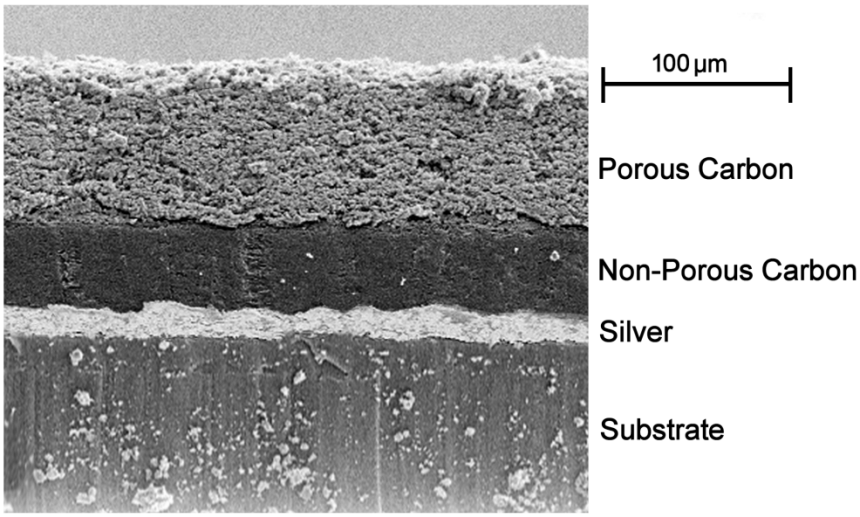

Figure 4. *A scanning electron microscope image of a cross section of a screen-printed porous carbon electrode having a low IR-drop. (From N. J. van Dijk [29])*

Areal Capacitance

The areal capacitance of carbon electrodes depends strongly on carbon type. Graphite is the simplest case to consider, because it lacks surface functionalities. In this special case, the areal capacitance may be represented, to a first approximation, as the weighted sum

$$C_{\text{total}} = \theta \hat{C}_{\text{basal}} + (1-\theta)\hat{C}_{\text{edge}}$$

where C_{total} is the total areal capacitance, and $\hat{C}_{\text{basal}}$ and $\hat{C}_{\text{edge}}$ are the *areal capacitance components* of the basal plane and the edge plane respectively. Rough estimates, in strong electrolyte solutions, are $\hat{C}_{\text{basal}} = 2\ \mu\text{F cm}^{-2}$, and $\hat{C}_{\text{edge}} = 70\ \mu\text{F cm}^{-2}$. (The idea that the capacitance of carbon can be decomposed in this way seems to have originated in the work of Randin and Yeager [35], and Rice and McCreery [36].)

By contrast, activated carbon, like glassy carbon, has multiple surface functionalities which vary with provenance and pre-treatment. Typically, these functionalities are oxygen-type and undergo reversible Faradaic reactions which manifest as a very large "pseudo-capacitive" component $\hat{C}_{\text{pseudo}} \approx 400\ \mu\text{F cm}^{-2}$ in the total response. For some applications (e.g. supercapacitors) it is actually desirable to increase the pseudo-capacitive component. However, because the surface coverage of oxygen functionalities is sterically restricted to ~25% by the need for them to be covalently attached to the carbon substrate, the maximum

areal capacitance is ~100 μF cm^{-2} on a flat electrode surface, and is often only one fifth of that. For other applications, such as anodic stripping voltammetry on glassy carbon electrodes, functionality-free surfaces are preferred. These typically have areal capacitances in the range 2-10 μF cm^{-2}.

The origin of the high capacitance of edge plane carbon (70 μF cm^{-2}) is somewhat mysterious, but may be due to a locally-enhanced population of charge carriers inside the lattice edges. On the other hand, the surprisingly low capacitance component of basal plane carbon (2 μF cm^{-2}) is almost certainly due to the presence of a space charge capacitance (C_{SC}) in series with the capacitance in solution:

$$C_{\text{basal}}^{-1} = C_{\text{sc}}^{-1} + C_{\text{solution}}^{-1}$$

Equivalent Circuit

Recently, a new equivalent circuit was proposed for porous carbon electrodes (Fig. 5). Naively, one might suppose that this would involve multiple ladder networks in parallel, in order to model the response of multiple pores in parallel. However, the somewhat surprising result is that the circuit in Fig. 5 is able to capture the complete multi-pore behaviour [37].

The equivalent circuit shown in Fig. 5 explains the three most striking properties of large-area carbon electrodes, namely their propensity to exhibit voltage decay at open circuit, their loss of equivalent series capacitance at high frequency, and their voltammetric distortion at high scan rate. It also explains the shape of observed complex plane impedance plots over the entire frequency range. For screen-printed porous carbon electrodes (whether in aqueous, organic, or ionic liquid solution) one generally finds that the solitary *RC*-parallel network on the right-hand side of Fig. 5 dominates the impedance response at high frequencies (>1 kHz, say), because this corresponds to the resistance of the electrolyte solution. In contrast, the vertical ladder network dominates the impedance response at low frequencies. In the latter case, the time constants of the “rungs” of the ladder network correspond to charge/discharge phenomena deep inside pores, and empirically these are found to occur over many orders of magnitude, from milliseconds to kiloseconds.

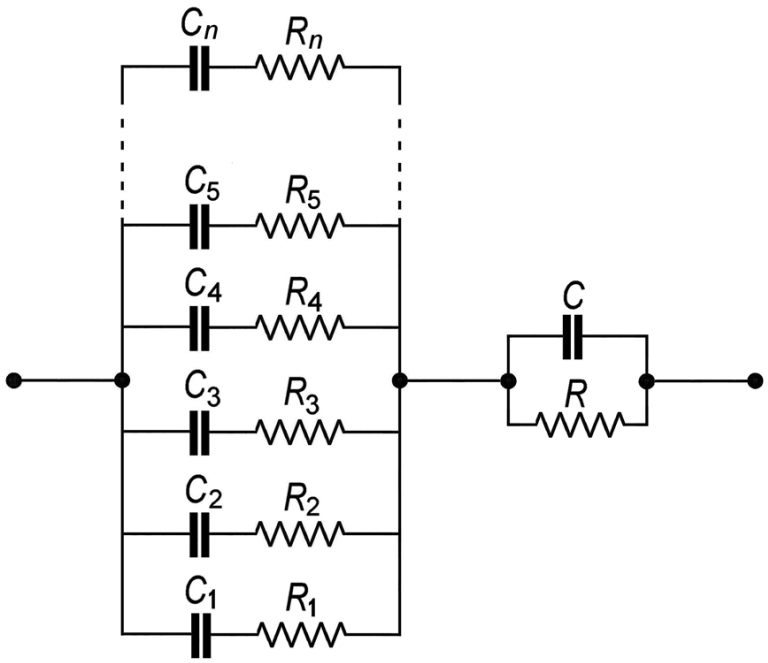

Figure 5. *The equivalent circuit of a porous carbon electrode. It consists of a single vertical ladder network in series with an RC parallel network. The ladder network models the response of pores in the body of the electrode, whereas the solitary RC parallel network models the response of the electrolyte solution. (In many cases, the capacitance of the electrolyte solution is better represented as a constant phase element.)*

Finally, it should be noted that the resistance of all graphitic carbons is generally insignificant compared with the resistance of their liquid-filled pores, so it is the liquid-filled pores that determine the *RC* time constants in the system. For example, the room-temperature conductivity of activated carbon is about 0.06×10^{3} S/cm, whereas the room-temperature conductivity of aqueous sulfuric acid at its conductivity maximum (31 wt %) is 830×10^{-3} S/cm. Hence, even in this extreme case, the pore channels containing sulfuric acid are more resistive than the pore walls by a factor of circa 70. The ratio is even more extreme in the case of organic solvents and ionic liquids.

References

[1] J. P. Hart and S. A. Wring. *Recent developments in the design and application of screen-printed electrochemical sensors for biomedical, environmental and industrial analyses*. TrAC Trends in Analytical Chemistry 16, 89-103 (1997).

[2] J. Wang, B. Tian, V. B. Nascimento, and L. Angnes. *Performance of screen-printed carbon electrodes fabricated from different carbon inks*. Electrochimica Acta 43, 3459-3465 (1998).

[3] S. Kröger, A. P. F. Turner, K. Mosbach, and K. Haupt. *Imprinted polymer-based sensor system for herbicides using differential-pulse voltammetry on screen-printed electrodes*. Analytical Chemistry 71, 3698-3702 (1999).

[4] M. Albareda-Sirvent, A. Merkoçi, and S. Alegret. *Configurations used in the design of screen-printed enzymatic biosensors. A review*. Sensors and Actuators B: Chemical 69, 153-163 (2000).

[5] K. C. Honeychurch and J. P. Hart. *Screen-printed electrochemical sensors for monitoring metal pollutants*. TrAC Trends in Analytical Chemistry 22, 456-469 (2003).

[6] Y. Lin, F. Lu, and J. Wang. *Disposable carbon nanotube modified screen-printed biosensor for amperometric detection of organophosphorus pesticides and nerve agents*. Electroanalysis 16, 145-149 (2004).

[7] J. Wang and M. Musameh. *Carbon nanotube screen-printed electrochemical sensors*. Analyst 129, 1-2 (2004).

[8] S. Carrara, V. V. Shumyantseva, A. I. Archakov, and B. Samorì. *Screen-printed electrodes based on carbon nanotubes and cytochrome P450scc for highly sensitive cholesterol biosensors*. Biosensors and Bioelectronics 24, 148-150 (2008).

[9] M. A. Alonso-Lomillo, O. Domínguez-Renedo, and M. J. Arcos-Martínez. *Screen-printed biosensors in microbiology; a review*. Talanta 82, 1629-1636 (2010).

[10] J. P. Metters, R. O. Kadara, and C. E. Banks. *New directions in screen printed electroanalytical sensors: an overview of recent developments*. Analyst 136, 1067-1076 (2011).

[11] J. Ping, J. Wu, Y. Wang, and Y. Ying. *Simultaneous determination of ascorbic acid, dopamine and uric acid using high-performance screen-printed graphene electrode.* Biosensors and Bioelectronics 34, 70-76 (2012).

[12] M. Li, Y-T. Li, D-W. Li, and Y-T. Long. *Recent developments and applications of screen-printed electrodes in environmental assays—A review*. Analytica Chimica Acta 734, 31-44 (2012).

[13] K. Jost, D. Stenger, C. R. Perez, J. K. McDonough, K. Lian, Y. Gogotsi, and G. Dion. *Knitted and screen printed carbon-fiber supercapacitors for applications in wearable electronics*. Energy & Environmental Science 6, 2698-2705 (2013).

[14] J. D. Bernal, and J. Mason. *Packing of spheres: co-ordination of randomly packed spheres*. Nature 188, 910-911 (1960).

[15] G. D. Scott, and D. M. Kilgour. *The density of random close packing of spheres*. Journal of Physics D: Applied Physics, 2, 863-866 (1969).

[16] E. P. Mamunya, V. V. Davidenko, and E.V. Lebedev. *Percolation conductivity of polymer composites filled with dispersed conductive filler*. Polymer composites, 16, 319-324 (1995).

[17] S. H. Foulger. *Electrical properties of composites in the vicinity of the percolation threshold.* Journal of Applied Polymer Science, 72, 1573-1582 (1999).

[18] R. E. Franklin. *Crystallite growth in graphitizing and non-graphitizing carbons*. Proceedings of the Royal Society of London. Series A. Mathematical and Physical Sciences 209, 196-218 (1951).

[19] M. Pumera, S. Sánchez, I. Ichinose, and J. Tang. *Electrochemical nanobiosensors*. Sensors and Actuators B 123, 1195-1205 (2007).

[20] S. Ito, and Y. Mikami. *Porous carbon layers for counter electrodes in dye-sensitized solar cells: Recent advances and a new screen-printing method.* Pure Appl. Chem., 83, 2089-2106 (2011).

[21] A. Bottino, G. Capannelli, S. Munari, and A. Turturro. *Solubility parameters of poly(vinylidene fluoride)*. Journal of Polymer Science Part B: Polymer Physics, 26, 785-794 (1988).

[22] http://www.wolframalpha.com/ (Champaign, IL, USA). Retrieved 01 August 2014.

[23] A. F. M. Barton, *Handbook of Solubility Parameters and other Cohesion Parameters*, 2nd Edition, CRC Press, Boca Raton (1983).

[24] D. R. Lide, *Handbook of Organic Solvents*. CRC Press (1994)

[15] J.-L. M. Abboud, R. Notario. *Critical compilation of scales of solvent parameters. Part I. Pure, non-hydrogen bond donor solvents – technical report*. Pure Appl. Chem. 71, 645-718 (1999).

[26] The Cosmetic Ingredient Review Panel. *Final Report on the Safety Assessment of Propylene Carbonate*. International Journal of Toxicology 6, 23-51 (1987).

[27] http://www.oehha.org *List of Chemicals as Known to the State of California to Cause Cancer or Reproductive Toxicity*. California OEHHA. Retrieved 24 November 2014.

[28] M. Li, I. Katsouras, C. Piliego, G. Glasser, I. Lieberwirth, P. W. M. Blom, and D. M. de Leeuw. *Controlling the microstructure of poly(vinylidene-fluoride)(PVDF) thin films for microelectronics*. Journal of Materials Chemistry C 1, 7695-7702 (2013).

[29] N. J. van Dijk, *Rapid prototyping of electrode materials for fuel cells*, PhD Thesis, Loughborough University (2005).

[30] J. A. Owczarek, and F. Howland. *A study of the off-contact screen printing process. I. Model of the printing process and some results derived from experiments*. IEEE Transactions on Components, Hybrids, and Manufacturing Technology, 13, 358-367 (1990).

[31] R. E. Trease and R. L. Dietz. *Rheology of pastes for thick film printing*. Solid State Technology,15, 39-43 (1972).

[32] A. N. Gent, and A. J. Kinloch. *Adhesion of viscoelastic materials to rigid substrates. III.* Energy criterion for failure. Journal of Polymer Science Part A2: Polymer Physics 9, 659-668 (1971).

[33] E. H. Andrews, A. J. Kinloch. *Mechanics of Adhesive Failure I.* Proc. R. Soc. Lond. A. 332, 385-399 (1973).

[34] E. H. Andrews, and N. E. King. *Surface energetics and adhesion*. pp 47-63, in Polymer Surfaces, Clark, D.T., and W. J. Feast, eds., John Wiley & Sons, Chichester, (1978).

[35] J-P. Randin, and E. Yeager, *Differential capacitance study on the basal plane of stress-annealed pyrolytic graphite*. J. Electroanal. Chem. 36, 257-276 (1972).

[36] R. J. Rice and R. L. McCreery, *Quantitative Relationship between Electron Transfer Rate and Surface Microstructure of Laser-Modified Graphite Electrodes*. Anal. Chem., 61, 1637-1641 (1989).

[37] S. Fletcher, V. J. Black, and I. Kirkpatrick, *A Universal Equivalent Circuit for Carbon-based Supercapacitors*, Journal of Solid State Electrochemistry, 18, 1377-1387 (2014).